Applied Catalysis B: Environmental 136–137 (2013) 56–63

Contents lists available at SciVerse ScienceDirect

Applied Catalysis B: Environmental

journal homepage: www.elsevier.com/locate/apcatb

TiO_2/Cu(II) photocatalytic production of benzaldehyde from benzyl alcohol in solar pilot plant reactor

Danilo Spasiano[a,*], Lucia del Pilar Prieto Rodriguez[b], Jaime Carbajo Olleros[c], Sixto Malato[b], Raffaele Marotta[a], Roberto Andreozzi[a]

[a] Dipartimento di Ingegneria Chimica, dei Materiali e della Produzione Industriale, Università di Napoli "Federico II", p.le V. Tecchio 80, 80125 Naples, Italy
[b] Plataforma Solar de Almería-CIEMAT, Carretera de Senés Km 4, 04200 Tabernas, Almería, Spain
[c] Departamento de Ingeniería de Procesos Catalíticos Instituto de Catálisis y Petroleoquímica, CSIC, C/Marie Curie 2, 28049 Cantoblanco, Madrid, Spain

ARTICLE INFO

Article history:
Received 27 November 2012
Received in revised form 14 January 2013
Accepted 19 January 2013
Available online 7 February 2013

Keywords:
Selective oxidation
Benzyl alcohol
Benzaldehyde production
TiO_2 photocatalysis
Solar photocatalytic plant
Figure-of-merit

ABSTRACT

The technical feasibility of selective photocatalytic oxidation of benzyl alcohol to benzaldehyde, in aqueous solutions, in presence of cupric ions has been investigated in a solar pilot plant with Compound Parabolic Collectors. Aldrich (pure anatase) and P25 Degussa TiO_2 have been used as photocatalysts. The influences of cupric species concentrations, solar irradiance and temperature are discussed too. The oxidation rates were strongly influenced by the initial cupric ions concentration, incident solar irradiance and temperatures.

The best results found, in terms of yields and selectivities to benzaldehyde under acidic conditions were higher than 50% and 60%, respectively, under acidic conditions.

Under deaerated conditions, the presence of reduced copper species was proved by XPS analysis. The results indicated that, at the end of the process, cupric species can be easily regenerated and reused, through a re-oxidation of reduced copper, produced during the photolytic run, with air or oxygen in dark conditions.

A figure-of-merit (A_{CM}), proposed by the International Union of Pure and Applied Chemistry (IUPAC) and based on the collector area, has been estimated, under the proposed conditions, with the aim to provide a direct link to the solar-energy efficiency independently of the nature of the system. Generally speaking, it can be considered that the lower A_{CM} values the higher the system efficiency.

1. Introduction

The use of TiO_2, as readily available and environmentally friendly photocatalyst, was largely investigated for the removal of non-biodegradable or undesiderable organic substances from wastewater [1–3] and TiO_2 based on solar technologies were developed during the past years for reducing the cost of large-scale aqueous-phase applications to treat industrial wastewater [4,5]. However, only in recent years the research has pointed its attention on the possibility to use the TiO_2 as a photocatalyst for the selective oxidation of organic molecules under UV radiation in non-aqueous media [6]. For example, the selective oxidation of aromatic alcohols in the respective aldehydes can be easily gained in acetonitrile or in solvent free systems at room temperature [7,8] due to the reaction of the alcoholic substrate with the photogenerated positive holes (h_{VB}^+) and using oxygen as acceptor of photoelectrons [9]. In particular, the addition of an organic solvent, as acetonitrile, allows the oxidation of benzyl alcohol and its derivates with selectivities to the respective aldehydes of over 90% [8,10], values well higher than those reported (10–60%) when the same process is carried out in aqueous solutions using TiO_2 nanoparticles [11,12].

Moreover, selectivities of 41–74% were reported for the oxidation of 4-substituted aromatic alcohols to the corresponding aldehydes, using aqueous media, over rutile or anatase TiO_2 catalysts [11,13]. The decrease of the selectivity in aqueous solution with respect the use of organic non-aqueous solvent is mainly due to [9]:

(a) formation of very reactive species such as hydroxyl radicals ($HO^\bullet$) through the reaction of adsorbed water molecules or hydroxyl groups with positive holes:

$$H_2O_{ads}/HO_{ads}^- \xrightarrow{h_{(VB)}^+} HO^\bullet + H^+ \quad (r_1)$$

(b) generation of radical superoxide ($O_2^{\bullet-}$) by the reaction of molecular oxygen with photogenerated electrons (r_2). In presence of water, $O_2^{\bullet-}$ species gives rise to hydrogen peroxide

* Corresponding author. Tel.: +39 0817682968; fax: +39 0815936936.
E-mail address: danilo.spasiano@unina.it (D. Spasiano).

0926-3373/$ – see front matter © 2013 Elsevier B.V. All rights reserved.
http://dx.doi.org/10.1016/j.apcatb.2013.01.055

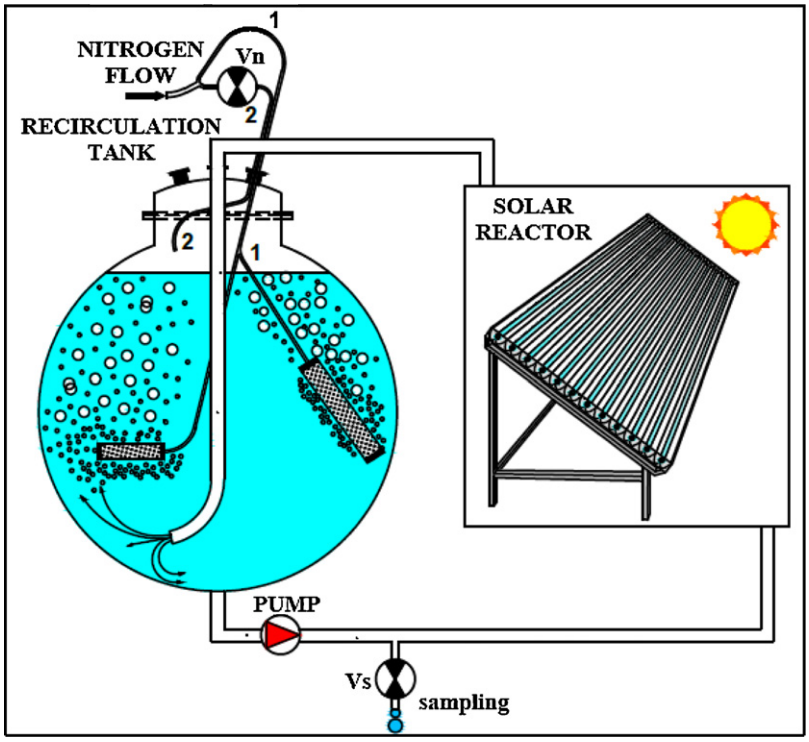

Fig. 1. Solar photocatalytic CPC pilot plant reactor.

(r_3) whose electron trapping generates HO• radicals (r_4), which oxidizes not selectively the organic substances (r_5):

$$O_{2\,ads} \xrightarrow{e_{(CB)}^-} O_{2\ ads}^{\bullet -} \quad (r_2)$$

$$O_{2\,ads}^{\bullet -} + 2H^+ \xrightarrow{e_{(CB)}^-} H_2O_{2\,ads} \quad (r_3)$$

$$H_2O_{2\,ads} \xrightarrow{e_{(CB)}^-} HO^{\bullet} + HO^- \quad (r_4)$$

$$HO^{\bullet} + S \rightarrow S_{ox} \quad (r_5)$$

On the other side, water is considered the best solvent for environmental friendly process and, for this reason, other new approaches have arisen in order to avoid the use the organic solvents. In particular, very recent studies demonstrated that the use of Cu(II) ions, as electron acceptor, instead of molecular oxygen, under deaerated conditions, leads to an increase of selectivity to benzaldehyde up to 72%, starting from benzyl alcohol [14], since the formation of hydroxyl radicals takes place just by the reaction of water molecules or surface adsorbed hydroxyl groups with positive holes. In this case, cupric ions reduce to a lower state of oxidation by capturing the photogenerated electron on the TiO_2 surface and precipitate from the solution:

$$Cu(II) \xrightarrow{e_{(CB)}^-} Cu(I) \xrightarrow{e_{(CB)}^-} Cu(0) \quad (r_6)$$

whereas adsorbed benzyl alcohol (BA) is oxidized to the benzaldehyde (BHA), through a direct reaction with the positive holes:

$$BA_{ads} \xrightarrow{2h_{(VB)}^+} BHA_{ads} \quad (r_7)$$

At the end of the process, cupric ions could be regenerated and reused, through the reoxidation of zero valent precipitated copper with an air flow at dark conditions.

Chemical state of solid copper after the photocatalytic run was also intensively investigated, but controversial results were reported. Most of the researchers reported that the solid is composed by a mixture of zero valent copper and cupric oxide (and, in some case, cuprous oxide) [15–19].

In some studies it was concluded that the reduced Cu species was zero valent copper [20,21]. However, the possibility of the presence of both Cu(I)/Cu(II) species, due to a reoxidation of metal copper during the preparation of the analytical samples, was not completely ruled out [22].

At best of the authors' knowledge, only lab-scale lamp-driven investigations on the selective TiO_2 photocatalytic oxidation of benzyl alcohol and its derivatives, in aqueous or acetonitrile or solvent free systems, were reported in the literature [11,12,14,23–27].

It could be very interesting, for economic and environmental reasons, to evaluate the possibility of exploiting the use of solar radiations daily arriving on the earth surface, through the use of pilot plants, for the production of benzaldehyde from benzyl alcohol.

In the present work, the development of the TiO_2/Cu(II)/solar radiation system for the selective oxidation of benzyl alcohol to benzaldehyde in water is studied, by using a solar photocatalytic pilot plant at different operating conditions (TiO_2 photocatalyst type, Cu(II) initial concentration and irradiance of solar radiation). The possibility of reuse copper as catalyst is also tested by oxidizing the precipitated zero valent copper with an air flow blown into the pilot plant in dark conditions. Optimal conditions of TiO_2 load and pH values are fixed according to the ones found in previous studies [14,28].

Moreover, analyses of solid, after the oxidation runs, are carried out to better clarify the nature of copper species at the end of the process.

2. Materials and methods

2.1. Experimental set-up and procedures

2.1.1. Pilot plant experiments

Experimental investigations were carried out, from May to July 2012, in a solar pilot plant consisting of twelve Compound Parabolic

Collectors (CPC), installed in the Plataforma Solar de Almería (37° latitude N, Spain) and elsewhere described in its geometrical and functional characteristics [29]. The total solution volume is 39 l, where only 22 l are exposed to solar radiation; the rest is distributed between the recirculation tank (9 l) and the hydraulic connections (8 l). The recirculation tank of the adopted CPC was modified, as reported in Fig. 1, in order to ensure the absence of oxygen, essential for performing the proposed process. For this purpose, the solutions, containing the catalysts and the substrate, were preventively purged with nitrogen gaseous stream through two porous ceramic spargers, by closing the valve V_n, to remove the dissolved oxygen. During the experimental runs a continuous nitrogen flow was guaranteed to the reactor to prevent the entry of air in the reactor but it was switched in the freeboard of the recirculation tank, by opening the valve V_n, to inhibit the stripping of organic substances from the solution. In the last case, the bubbling of nitrogen is strongly limited by the pressure drop due to the spargers.

To better follow the concentration profiles of the compounds involved in the process, some experimental runs were carried out during two days. In these cases, at the end of the first day, the irradiated part of the reactor was covered and the recycling tank was capped to stop the photochemical reactions and to prevent the entry of oxygen, respectively.

Samples were collected in a glass bottle at different reaction times, by opening the valve V_s, rapidly filtered to prevent the reoxidation of precipitate copper and finally analyzed.

All the experimental data were reported in function of the accumulated energy, per unit of volume (kJ/l), incident on the reactor at the corresponding time of the withdrawn sample (Q_n) [30]:

$$Q_n = Q_{n-1} + \Delta t_n \cdot \overline{UV}_n \cdot \frac{A_r}{V_t}; \quad \Delta t_n = t_n - t_{n-1} \tag{1}$$

where Q_{n-1} represent the accumulated energy (per unit of volume, kJ/l) taken during the experiment relative to the previous sampling; Δt_n, $\overline{UV}_n$ and V_t are, respectively, the elapsed time, the average UV-irradiance (measured by a global UV radiometer KIPP&ZONEN, model CUV 3 mounted on a platform tilted the same angle as the CPCs) which reaches the collector surface (A_r) between the two samplings and the total solution volume.

2.1.2. Laboratory-scale experiments

Experiments were carried out in a Suntest solar simulator (Suntest XLS+ photoreactor, Atlas) equipped with a 765–250 W/m^2 Xenon lamp (61–24 W/m^2 from 300 nm to 400 nm, 1.4×10^{20}–5.5×10^{19} photons/m^2 s) and a cooler to keep the temperature at 35 °C. The UV irradiation, in the range of 300–400 nm, was monitored by using a portable radiometer (Solar Light CO PMA 2100) fixed on the shaker inside the lamp influence zone, like shown in Fig. 2.

In this case, a volume of 700 ml of reacting solution was prepared in a 1-l flask and, after 30 min of stripping with nitrogen, was rapidly poured in ten cylindrical glass vials with the capacity of 42 ml and a diameter of 25 mm. The vials were rapidly closed with a screw cap, to prevent the entry of oxygen, and were simultaneously exposed to the lamp radiation and agitated by a shaker like shown in Fig. 2. The temperature was set at 35 °C. Each vial represented a sample to remove from the solar box at different reaction times. Once collected, all the samples were rapidly filtered and analyzed.

The pH of the solutions was adjusted at the value of 2.0, for all the runs, by using an aqueous solution of 85% of phosphoric acid.

2.2. Analytical methods

The concentrations of benzyl alcohol, benzaldehyde and benzoic acid at different reaction times were evaluated by HPLC analysis. For this purpose, the HPLC apparatus (Agilent 1100) was equipped with a diode array UV/vis detector (λ = 215, 230, 250 nm) and Phenomenex (Gemini 5u C18 150 mm × 3 mm) column, using a mobile phase flowing at 0.7 ml min^{-1}. The mobile phase was prepared by a buffer solution (A), H_2O (B) and CH_3CN (C). A linear gradient progressed from 15% C to 28% C and from 45% B to 32% B in 10 min with a subsequent re-equilibrium time of 3 min. One litre of buffer was made by 10 ml of phosphoric acid solution (5.05 M), 50 ml of methyl alcohol and water for HPLC.

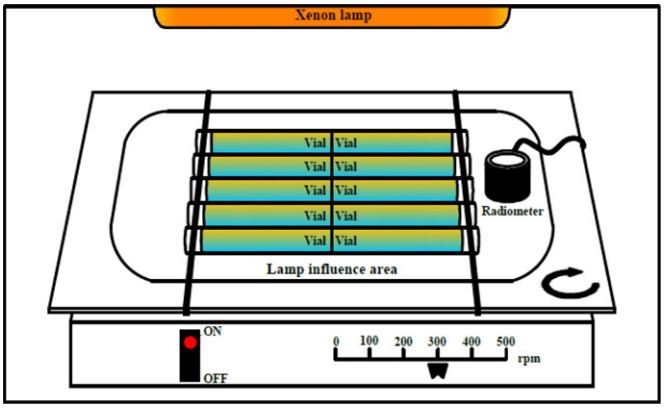

Fig. 2. Solar box.

The concentration of dissolved copper ions was measured by means of a colorimetric method using an analytical kit (based on oxalic acid bis-cyclohexylidene hydrazide, cuprizone®) purchased from Macherey-Nagel. An UV/vis spectrometer (UNICAM-II spectrophotometer) has been used for the measurements at a wavelength of 585 nm.

Total organic carbon (TOC) was monitored by Shimadzu Total Organic Carbon analyser model TOC-5050A, equipped with an auto sampler ASI 5000A. The pH was monitored by a portable pH-metre (Crison pH 25).

The Cu/Ti ratio for unknown solids, withdrawn at the end of some photocatalytic runs, was estimated by an Energy Dispersive X-ray spectrometer system (SwiftED, Oxford Instruments) attached to a Scanning Electron Microscope (TM-1000, Hitachi).

Powder X-ray diffraction (XRD) patterns were estimated using a XîPertPRO (PANalytical) diffractometer with nickel-filtered Cu Kα radiation. The X-ray generator was operated at 45 kV and 40 mA. The powders were scanned from $2\theta = 4°$ to 90° with a 0.02 step size and accumulating a total of 5 s per point.

X-ray photoelectron spectroscopy (XPS) analysis was carried out under high vacuum chamber with a base pressure below 9×10^{-7} Pa at room temperature. Photoemission spectra were recorded using a SPECS GmbH system equipped with an UHV PHOIBOS 150 analyser with Al monochromatic anode operated at 12 kV and 200 W with a photon energy of $h\nu$ = 1486.74 eV. A pass energy of 25 eV was used for high-resolution scans. Binding energies (BE) were referenced to C 1s peak (284.6 eV) to take into account charging effects.

The XPS spectra obtained were then curved fitted using the XPS PeakFit software. The areas of the peaks were computed by fitting the experimental spectra to Gaussian/Lorentzian curves after subtracting the background (Shirley function).

2.3. Materials

Two commercial microcrystalline TiO_2 powders were tested: P25 Degussa TiO_2 (80% anatase, 20% rutile, BET specific surface area 50 m^2 g^{-1}) and TiO_2 Aldrich (pure anatase phase, BET specific surface area 9.5 m^2 g^{-1}).

Cupric ions were introduced in the system as anhydrous cupric sulphate (Sigma–Aldrich) with a purity >99.0% (w/w). Benzyl alcohol (BA), benzaldehyde (BHA) and benzoic acid (BAC), with a purity >99.0% (w/w), were purchased from Sigma Aldrich and used as received. Phosphoric acid with a purity 85% from Merck as used as received.

3. Results and discussion

3.1. Effect of TiO_2 type

The results obtained during different experimental runs of solar photo-oxidation of benzyl alcohol, with two different typologies of commercial TiO_2 samples, at the same load (200 mg/l), are shown in Fig. 3a and b.

The runs were carried out in two days. At the end of first day, when the reactor was covered, the UV-irradiances (wavelength 300–400 nm) and temperatures decreased (see Fig. 3a and b). During the runs, measured UV-irradiances ranged between 40 and 50 W/m^2 approximately (Fig. 3b, continuous and dashed lines).

As shown in the diagrams, the reactivity of the system is higher when TiO_2 P25 by Degussa is used than the TiO_2 Aldrich catalyst. In particular, in presence of P25 Degussa sample (empty symbols), for a Q_n value of 123 kJ/l, the BA concentration approached to zero (Fig. 3a) and Cu(II) ions were totally reduced (Fig. 3b), whereas, if Aldrich TiO_2 sample is used (full symbols), about 27% of initial benzyl alcohol and Cu(II) ions were still present in the solution.

The higher reactivity observed for the system in presence of P25 Degussa TiO_2 is in disagreement with the results, previously reported [14], that show a similar reactivity when P25 Degussa and Aldrich TiO_2 catalysts were used in presence of an UV radiation emitted by a laboratory thermostated lamp.

This discrepancy may be probably due to the different emission spectra between lamp and the sun and (different) light absorption characteristics, in the range of 300–800 nm, of the two used catalysts.

Moreover, the different reactivities, recorded in the solar experiments, could be also attributed to the differences between the averages of the measured temperatures: 38.6 °C and 34.3 °C for runs carried out in presence of P25 Degussa (dotted lines) and Aldrich TiO_2 (dashed and dotted lines) catalysts, respectively (Fig. 3a).

As shown in Fig. 4, the BA solar photocatalytic oxidation resulted in the production of BHA (diamonds) for Aldrich (full symbols) and P25 Degussa (empty symbols) TiO_2 catalysts, and BAC an undesired product that derives from the reaction between the positive photogenerated holes on the TiO_2 surface and benzaldehyde. BAC yields are also reported in the same figure (triangles).

According to the previous results, the highest BHA production rates were gained in presence of P25 Degussa TiO_2. Moreover, for this catalyst, the maximum BAC production rate was reached at the highest yields of BHA.

However, for accumulated energy values higher than 80 kJ/l, when the unconverted BA concentration was less than 20% of its initial concentration (Fig. 3a, empty squares), a decrease in BHA yield with respect of initial BA amount, from the value of 53.3% to 45.5%, was observed using P25 Degussa TiO_2 samples. This result can be explained by considering a competition in the reaction between the BA and BHA molecules for the photogenerated positive holes on the TiO_2:

$$BA_{ads} \xrightarrow{2h_{(VB)}^{+}} BHA_{ads} \xrightarrow{2h_{(VB)}^{+}} BAC \qquad (r_8)$$

It is interesting to remark that for accumulated energy values higher than 120 kJ/l, in the case of Degussa TiO_2 catalyst, when Cu(I)/Cu(II) species are totally reduced (Fig. 3b, empty squares), being the

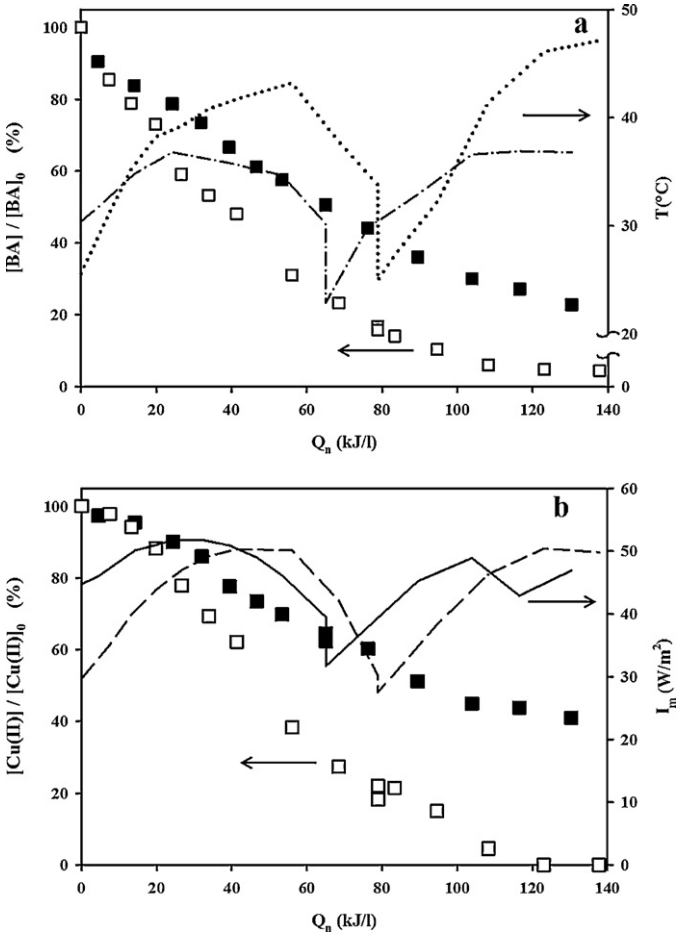

Fig. 3. Effect of TiO_2 type at pH 2.0: BA solar photoxidation (squares) and temperatures profiles (dotted and dashed-dotted lines) (a); Cu(II) solar photoreduction (squares) and UV-irradiance (continuous and dashed lines) (b). $[BA]_o$ = 1.5 mM. $[Cu(II)]_o$ = 1.5 mM. Initial TiO_2 load = 200 mg/l. (a) (■, -•-) Aldrich TiO_2, (□, •••) P25 Degussa TiO_2. (b) (■, ---) Aldrich TiO_2, (□, —) P25 Degussa TiO_2.

predominant reaction the recombination between photoinduced positive holes and electrons:

$$h_{(VB)}^{+} + e_{(CB)}^{-} \rightarrow \text{heat} \qquad (r_9)$$

the BA (Fig. 3a, empty squares) and BHA (Fig. 4, empty diamonds) consumption and BAC production rates (Fig. 4, empty triangles) stopped.

The BHA selectivity, with respect to BA consumption, was calculated for both TiO_2 types (Fig. 5). As shown in the diagram, it seems that the use of Aldrich TiO_2 sample renders the system more selective, reaching, for Q_n values of 130 kJ/l, BHA selectivity values close to 70% (in presence of P25 Degussa, only a value of 50% was obtained).

The highest selectivity achieved in presence of Aldrich TiO_2 sample is correlated at the lower degree of conversion (Fig. 3a, full squares) when compared with the test in which P25 Degussa is used (Fig. 3a, empty squares).

TOC measurements collected during the runs are also reported in Fig. 5, in terms of mineralization degrees. Due to the HO radicals generation from the reaction of water molecules or surface adsorbed hydroxyl groups with positive holes [37]:

$$(H_2O)_{ads} + h_{VB}^{+} \rightarrow HO^{\bullet} + H^{+} \qquad (r_{10})$$

$$(HO^{-})_{ads} + h_{VB}^{+} \rightarrow HO^{\bullet} \qquad (r_{11})$$

the two trends are very similar, with a degree of mineralization at the end of the experimental runs of 9% and 7% in presence of P25

Degussa and Aldrich TiO_2 respectively, However, the low degree of mineralization achieved demonstrates the possibility of using such system to carry out selective oxidations in aqueous media.

3.2. Effect of cupric ions concentration

To evaluate the effect of Cu(II) initial concentration, some experimental runs of solar photoxidation of benzyl alcohol were carried out with Aldrich TiO_2 at the load of 200 mg/l and pH 2.0, varying the cupric ions starting concentration (0.5 mM, 1.0 mM and 1.5 mM).

As shown in Fig. 6a and b, the temperatures and UV-irradiances profiles (solid, dashed and dotted lines) are so similar as to be considered equals for the three runs.

With Cu(II) and BA starting concentrations of 0.5 mM and 1.5 mM, respectively, the BA oxidation stopped for Q_n values close to 35 kJ/l where a complete reduction of cupric ions was observed (full triangles).

At the highest Cu(II) initial concentration (1.5 mM), it resulted into a decrease of the system reactivity and BA conversion (Fig. 6a, full circles) and, at the same time, the Cu(II) reduction rates decrease. The observed results, according to those previously reported [14], are probably due to a partial catalyst deactivation by

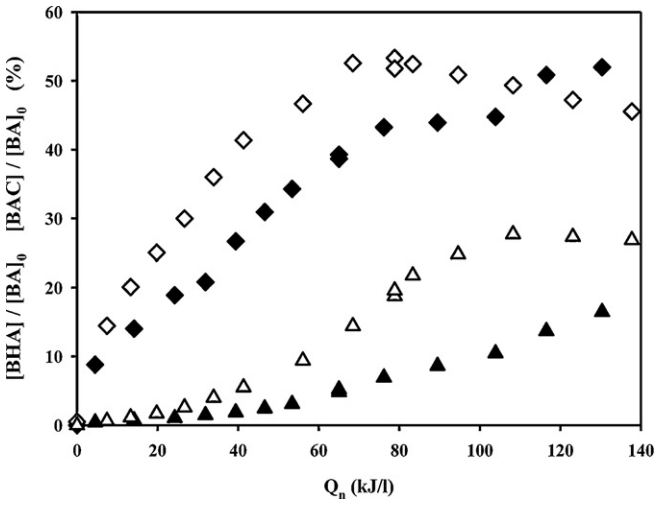

Fig. 4. Effect of TiO_2 type on the BHA and BAC production. $[BA]_o$ = 1.5 mM. $[Cu(II)]_o$ = 1.5 mM. Initial TiO_2 load = 200 mg/l. pH 2.0. Aldrich TiO_2: ♦ BHA, ▲ BAC. P25 Degussa TiO_2: ◊ BHA, △ BAC.

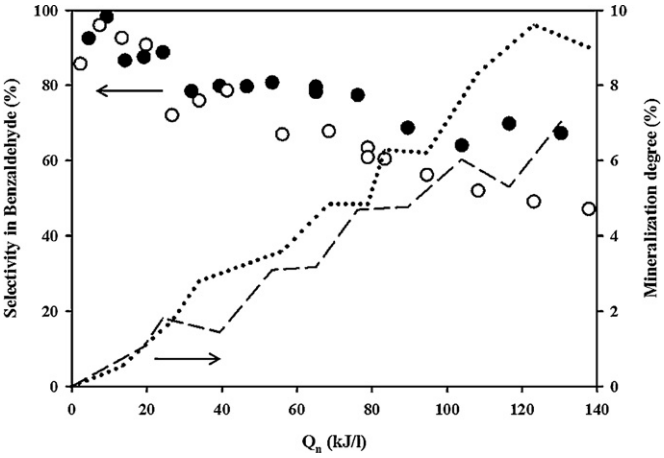

Fig. 5. Effect of TiO_2 type on the BHA selectivity and mineralization degree (dotted and dashed lines). $[BA]_o$ = 1.5 mM. $[Cu(II)]_o$ = 1.5 mM. Initial TiO_2 load = 200 mg/l. pH 2.0. Aldrich TiO_2: (●) BHA selectivity, (—) mineralization degree. P25 Degussa TiO_2: (○) BHA selectivity, (•••) mineralization degree.

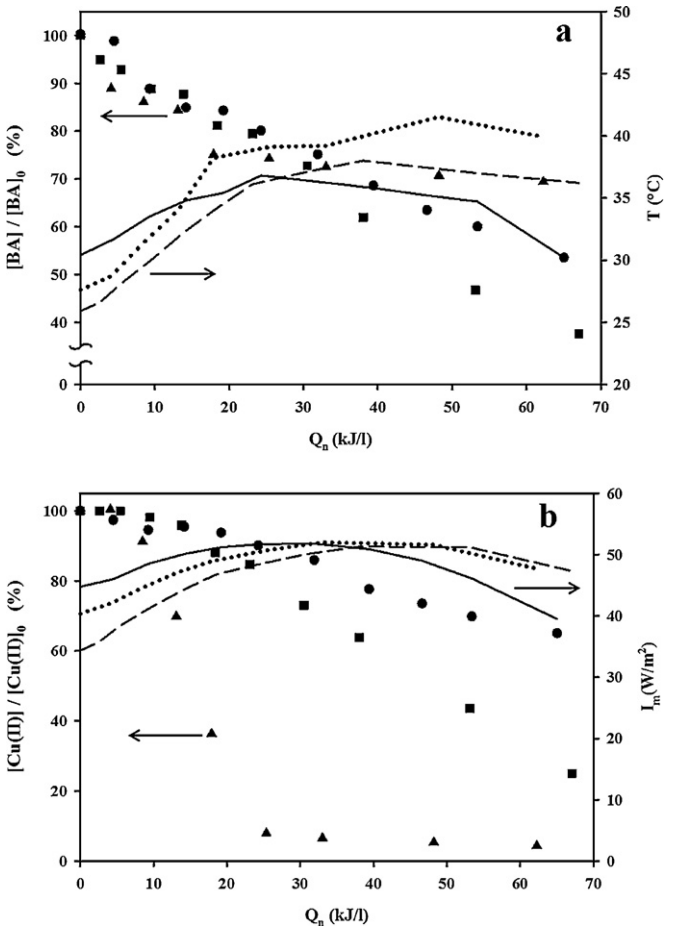

Fig. 6. Effect of initial Cu(II) concentration at pH 2.0 on the BA and Cu(II) concentration profiles: BA solar photoxidation and temperatures profiles (a); Cu(II) solar photoreduction and UV-irradiances profiles (b). $[BA]_o$ = 1.5 mM. Initial TiO_2 (Aldrich) load = 200 mg/l. $[Cu(II)]_o$: (▲) 0.5 mM, (■) 1.0 mM, (●) 1.5 mM. Temperatures and irradiances: (•••) for $[Cu(II)]_o$ = 0.5 mM, (—) for $[Cu(II)]_o$ = 1.0 mM, (---) for $[Cu(II)]_o$ = 1.5 mM.

the adsorbed sulphate ions which may block the TiO_2 active sites (s*) [31]:

$$SO_4^{2-} + s* \rightleftharpoons SO_{4(ads)}^{2-} \qquad (r_{12})$$

In fact, since Cu(II) species were added to the reactive solution as cupric sulphate ($CuSO_4$), increasing the Cu(II) ions initial concentration results into an increase of sulphate concentration too.

Moreover, the sulphate anions, at concentration level higher than 1.0 mM, exerted a negative effect, inhibiting the BA photooxidation rates because they are in competition with BA molecules in the reaction with the positive holes [14]:

$$SO_4^{2-} + h_{VB}^{+} \rightarrow SO_4^{\bullet -} \qquad (r_{13})$$

In Fig. 7 are reported the experimental concentration profiles of BHA and BAC (full and empty symbols) that are in agreement with BA concentration trends shown in Fig. 6a. In particular the best result found, in term of yield, was of 43% for BHA, starting with $[Cu(II)]_o$ = 1.0 mM, for a accumulated energy value of 67 kJ/l. For all the runs, the selectivity was always higher than 67% and the mineralization degrees were lower than 4.5% (data not shown).

3.3. Effect of the irradiance and temperature

As previously shown in Figs. 3b and 6, the Cu(II) concentrations are characterized by a s-shaped profile and, in particular, when the

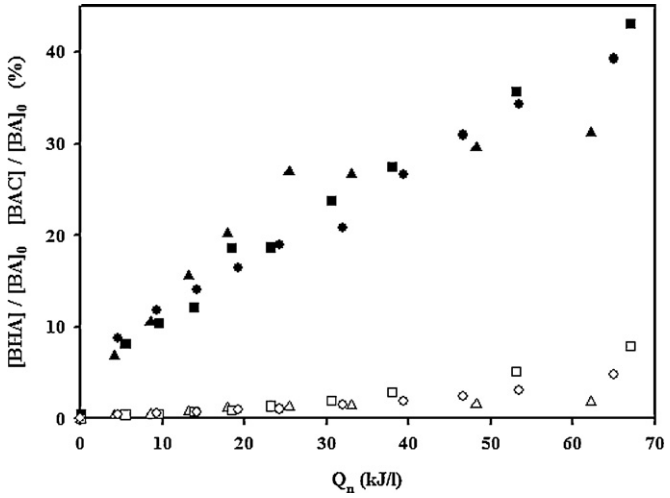

Fig. 7. Effect of initial Cu(II) concentration on the BHA and BAC concentration profiles: BHA (full symbols) and BAC (empty symbols) productions. $[BA]_o$ = 1.5 mM. Initial TiO_2 (Aldrich) load = 200 mg/l, pH 2.0. $[Cu(II)]_o$: (▲, △) 0.5 mM, (■, □) 1.0 mM, (●, ○) 1.5 mM.

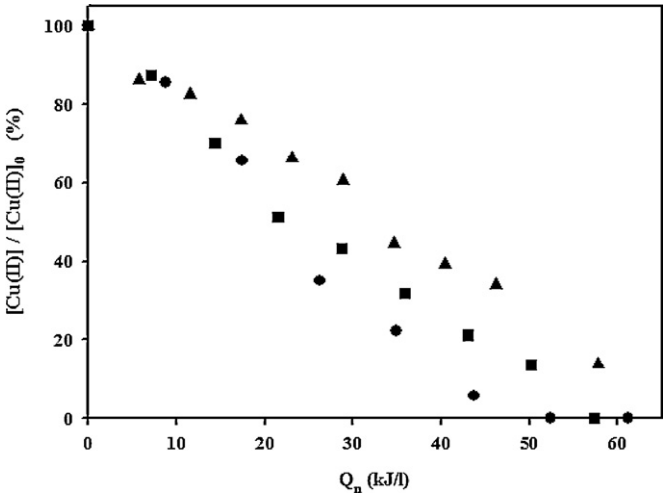

Fig. 8. Effect of irradiance on the Cu(II) concentration profiles: $[BA]_o$ = 1.5 mM. $[Cu(II)]_o$ = 0.5 mM. Initial TiO_2 (Aldrich) load = 258 mg/l, pH 2.0 and T = 35 °C. UV irradiance (solar box): ▲ 39.5 W/m², ■ 49.0 W/m², ● 59.7 W/m².

solar UV radiations and reactor temperatures reached the top, a marked increase of Cu(II) reduction rate was observed. With the aim to better assess the relationship between the variability of both irradiances and temperatures during a solar run and the s-shaped of cupric ions concentration profile, a set of three laboratory photolytic experiments, with Cu(II) initial concentration equal to 0.5 mM, were carried out at three different irradiances, kept constant during a single run and under controlled solution temperature (T = 35 °C). For this purpose, a solar box apparatus, described in the experimental section, was used. Since the internal diameters of CPC solar reactor tubes and the solar box vials are 31 mm and 24 mm respectively, the TiO_2 load that maximizes the adsorption of UV radiation emitted by solar lamp is higher than that used for solar experiments carried out in CPC reactor.

The optimum TiO_2 concentration (c_{cat}), for which the optical thickness equals that of CPC reactor configuration (τ = 9.12) can be easily calculated as suggested by others [28,32]:

$$c_{cat} = \frac{\tau}{(\sigma + k) \times d} = 258 \quad \text{mg/l} \tag{2}$$

where σ is the scattering coefficient (1.295×10^3 m²/kg), k is the catalyst specific mass absorption (1.75×10^2 m²/kg) and d the internal tube diameter (24 mm).

As shown in Fig. 8, by increasing the UV irradiance from 39.5 W/m² to 59.7 W/m², the Cu(II) photoreduction rate increases.

A parallel increase of BA oxidation rate was also observed (data not shown). The results collected during these runs indicate that, under controlled temperature and irradiance, no s-shaped concentration profile was recorded.

3.4. Figure-of-merit

To estimate the operating costs of sole natural radiation, the figure-of-merit concept was used [33]. For solar-energy-driven systems, the figure-of-merit allows the assessment of the solar technology efficiency used for the investigated process. In fact, even if there is no cost for solar radiation, there could be a non-marginal capital cost for the collector. Being the capital cost of a solar collector generally proportional to its area, a figure-of-merit, based on the solar collector area, is appropriate.

For the adopted experimental batch conditions, the appropriate figure-of-merit is the collector area per mass (A_{CM}), defined as the collector area required to reduce of a unit mass of the substrate in the reacting system in a time of 1 h (t_o) for an incident solar irradiance of 1000 W/m² (E_S^o):

$$A_{CM} = \frac{1000 \cdot A_r \cdot t \cdot \overline{E_S}}{M \cdot V_t \cdot t_o \cdot \overline{E_S^o} \cdot (c_i - c_f)} \tag{3}$$

where A_r (3.19 m²) is the real collector area, M is the molar mass of the substrate (108.14 g/mol), V_t (39 l) is the volume of treated solution, $\overline{E_S}$ (814.6 W/m²) is the average direct solar irradiance over the reaction time t (4.83 h), c_i and c_f are, respectively, the initial and final substrate concentrations (mol/l), E_S^o is the standardized irradiance (1000 W/m², based on the AM1.5 standard solar spectrum on a horizontal surface) [34] and t_o is the reference time (1 h).

On the basis of the previous formula an average value of $A_{CM} = 3.08 \times 10^3$ m² per kilogram of benzyl alcohol and per hour consumed was thus calculated for the collector area per mass (200 mg/l of Aldrich TiO_2, pH 2.0, $[Cu(II)]_0$ = 1.0 mM, $[BA]_0$ = 1.5 mM).

3.5. Copper reuse

The possibility of reuse the reduced copper, as catalyst, was tested by carrying out an experimental run, by using the CPC solar reactor, consisting in three cycles of BA photo-oxidation (Fig. 9). When all Cu(II) species was totally reduced as precipitate copper,

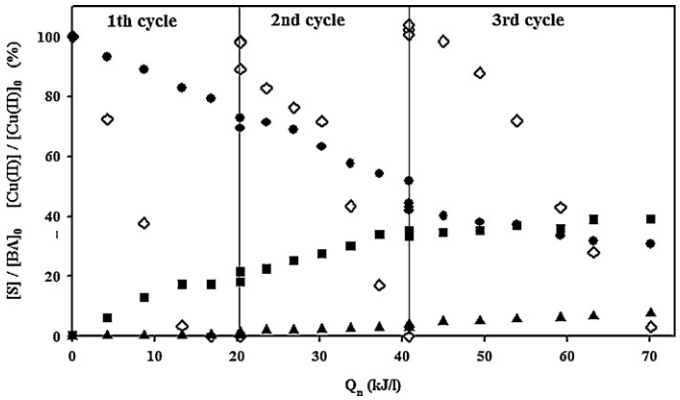

Fig. 9. Normalized concentration profiles for Cu(II), BA, BHA and BAC with light on and nitrogen purge or light off and oxygen purge. $[BA]_o$ = 2.5 mM. $[Cu(II)]_o$ = 0.5 mM. Initial TiO_2 (Aldrich) load = 200 mg/l, pH 2.0. ◊ Cu(II), ● BA, ■ BHA, ▲ BAC.

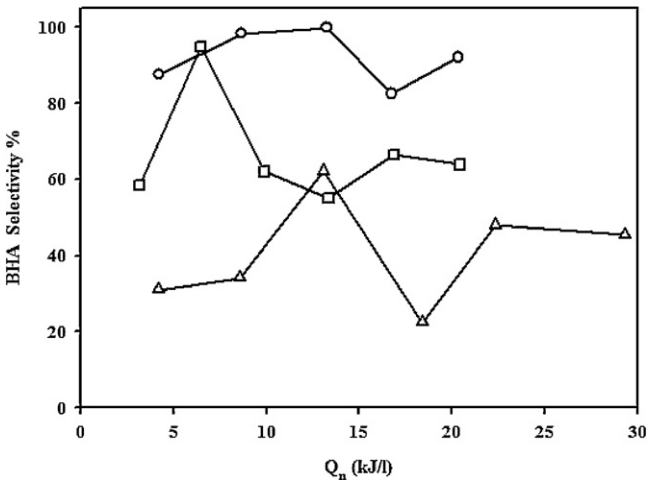

Fig. 10. BHA selectivities during the three cycles: $[BA]_o$ = 1.5 mM. $[Cu(II)]_o$ = 0.5 mM. Initial TiO_2 (Aldrich) load = 200 mg/l, pH 2.0. ○ 1st cycle, □ 2nd cycle, △ 3rd cycle.

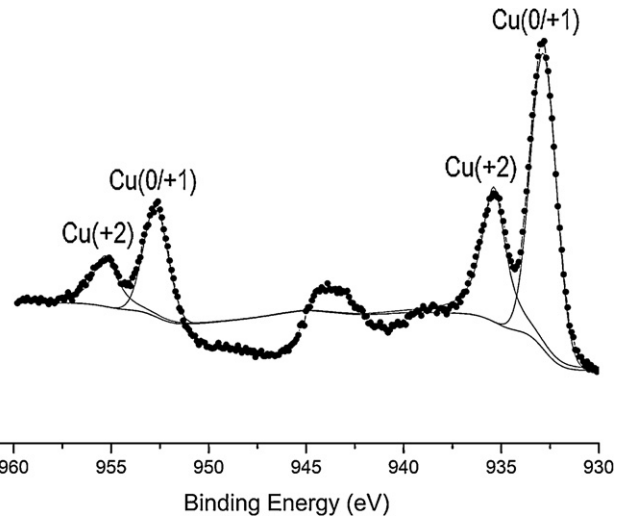

Fig. 11. XPS spectra for the solid sample after the photocatalytic oxidation run.

its reoxidation was carried out, in dark conditions, under air bubbling in the recirculation tank for 30 min. At the end of the first cycle, the reactive solution was re-purged with nitrogen gas, for other 30 min, to remove the dissolved oxygen and a new photocatalytic cycle was started. The experimental results, reported in Fig. 9, pointed out that it is possible, for each cycle, to reoxidize completely the precipitate copper to cupric species (empty diamonds).

During the first two cycles of BA solar photoxidation, not particular changes were observed on the reactivity of the system, whereas during the third cycle a decrease of both BA consumption and BHA production rates were observed. This behaviour could be explained by considering that the solution composition changes during the experimental run. In particular, at the 3rd cycle beginning, BA conversion and BHA yield were 43% and 33%, respectively, thus favouring a competition kinetics between BA and BHA, both adsorbed on TiO_2 surface, towards the reaction with the photogenerated holes [35]:

$$BA_{ads} + 2h^+ \xrightarrow{k=3.8\times10^5\ M/s} BHA_{ads}$$

$$BHA_{ads} + 2h^+ \xrightarrow{k=3.0\times10^4\ M/s} BAC_{ads}$$

The BHA selectivities of the process for the three photocatalytic cycles are reported in Fig. 10. As shown in the diagram, the highest selectivities (up to 100%) were obtained in the first cycle, whereas lower selectivities were observed during the second (close to 75%) and the third cycle (close to 40%), thus supporting, with the progress of the reaction time, the intervention of undesired oxidation reactions of BHA once produced.

After each photocatalytic cycle under anoxic conditions, the solid was filtered, stored under inert atmosphere and submitted to EDS, XRD and XPS analysis in order to better investigate the distribution of copper deposited on the solid and its oxidation states.

From the EDS investigations, Ti/Cu atom ratios, for the filtered solids, resulted 97.8/2.2, 96.5/3.5 and 85.2/14.8 (w/w) for the samples withdrawn at the end of the first, second and third cycle, respectively. These results supported the idea that reduced Cu species, formed during the photo-oxidative runs, accumulated on TiO_2 surface increasing the amount of deposited copper from the first cycle to third one up to 17.4% by weight. The increase of Cu amount on the TiO_2 is probably due to the deposition of a part of photocatalyst powders, during the experimental run, in the recirculation tank and/or along the hydraulic connections of the plant, thus decreasing the active load of it available in the solar photoreactor with a consequent reduction of BA consumption and BHA production rates, really observed, in particular during the third cycle.

A typical XPS spectra for the solid samples shows different peaks (Fig. 11). The peaks at 932.8 eV and 952.6 eV indicate the predominant presence of copper reduced species (+1/0) as previously reported by others [19,22,36] whereas the existence of peaks at 935.4 eV and 955.2 eV can be attributed to the presence of cupric species [22], such as CuO, probably an artefact produced during the preparation of the sample before the XPS analysis.

Unfortunately, XRD analysis did not give any result being the amount of Cu reduced species accumulated on the TiO_2 surface (max 17.4%) below XRD detection limit.

4. Conclusion

The possibility to convert benzyl alcohol to benzaldehyde by photocatalytic oxidation was demonstrated in aqueous solution under natural solar radiation at pilot plant scale. The oxidation rates were strongly influenced by the initial cupric ions concentration, incident solar irradiance and temperatures. The best result found, in terms of yield, was of 53.3% for benzaldehyde with respect to the initial benzyl alcohol concentration (63.4% of selectivity) for an accumulated energy value (Q_n) of 78.9 kJ/l (reaction time of 385 min) and operating with an average temperature of 38.6 °C.

EPS investigations, carried out on the solids, withdrawn during different photocatalytic cycles, confirmed the existence of both Cu reduced (0/+1) and oxidized species, the latter probably produced during the sample preparation before the analysis.

The results also indicated that cupric species can be easily regenerated and reused with air or oxygen in dark conditions.

A figure-of-merit (A_{CM}) was calculated be equal to 3.08×10^3 m^2 per kilogram and hour of benzyl alcohol converted.

References

[1] M.N. Chong, B. Jin, C.W.K. Chow, C. Saint, Water Research 44 (2010) 2997–3027.
[2] K. Rajeshwara, M.E. Osugi, W. Chanmanee, C.R. Chenthamarakshan, M.V.B. Zanoni, P. Kajitvichyanukul, R. Krishnan-Ayer, Journal of Photochemistry and Photobiology C: Photochemistry Reviews 9 (2008) 171–192.
[3] J.M. Herrmann, Applied Catalysis B: Environmental 99 (3/4) (2010) 461–468.
[4] R.J. Braham, A.T. Harris, Industrial & Engineering Chemistry Research 48 (2009) 8890–8905.
[5] S.R. Malato, P. Fernandez-Ibanez, M.I. Maldonado, G.J. Blanco, W. Gernjak, Catalysis Today 147 (2009) 1–59.
[6] Y. Shiraishi, T. Hirai, Journal of Photochemistry and Photobiology C: Photochemistry Reviews 9 (2008) 157–170.

[7] S. Higashimoto, N. Suetsugu, M. Azuma, H. Ohue, Y. Sakata, Journal of Catalysis 274 (2010) 76–83.
[8] W. Feng, G. Wu, L. Li, N. Guan, Green Chemistry 13 (2011) 3265–3272.
[9] C.S. Turchi, D.F. Ollis, Journal of Catalysis 122 (1990) 178–192.
[10] S. Higashimoto, N. Kitano, N. Yoshida, T. Sakura, M. Azuma, H. Ohue, Y. Sakata, Journal of Catalysis 266 (2009) 279–285.
[11] G. Palmisano, S. Yurdakal, V. Augugliaro, V. Loddo, L. Palmisano, Advanced Synthesis and Catalysis 349 (2007) 964–970.
[12] S. Yurdakal, G. Palmisano, V. Loddo, V. Augugliaro, L. Palmisano, Journal of American Chemical Society 130 (2008) 1568–1569.
[13] V. Augugliaro, V. Loddo, M.J. Lopez-Munoz, C. Marquez-Alvarez, G. Palmisano, L. Palmisano, S. Yurdakal, Photochemical & Photobiological Sciences 8 (2009) 663–669.
[14] R. Marotta, I. Di Somma, D. Spasiano, R. Andreozzi, V. Caprio, Chemical Engineering Journal 172 (2011) 243–249.
[15] J.W.M. Jacobs, F.W.H. Kampers, J.M.G. Rikken, C.W.T. Bulle-Lieuwma, D.C. Doningsberger, Journal of The Electrochemical Society 136 (1989), 2914-2023.
[16] M. Bideau, B. Claudel, L. Faure, M. Rachimoellah, Chemical Engineering Communications 93 (1990) 167–179.
[17] S. Morishita, Chemistry Letters 10 (1992) 1979–1982.
[18] N.S. Foster, R.D. Noble, C.A. Koval, Environmental Science & Technology 27 (1993) 350–356.
[19] S.W. Zou, C.W. How, J.P. Chen, Industrial & Engineering Chemistry Research 46 (20) (2007) 6566–6571.
[20] M. Canterino, I. Di Somma, R. Marotta, R. Andreozzi, Water Research 42 (2008) 4498–4506.
[21] H. Reiche, W.W. Dunn, A.J. Bard, Journal of Physical Chemistry 83 (1979) 2248–2251.
[22] S. Xu, J. Ng, A.J. Du, J. Liu, D.D. Sun, International Journal of Hydrogen Energy 36 (2011) 6538–6545.
[23] D.I. Enache, J.K. Edwards, P. Landon, B. Solsona-Espriu, A.F. Carley, A.A. Herzing, M. Watanabe, C.J. Kiely, D.W. Knight, G.J. Hutchings, Science 311 (2006) 362–365.
[24] S. Yurdakal, G. Palmisano, V. Loddo, O. Alagoz, V. Augugliaro, L. Palmisano, Green Chemistry 11 (2009) 510–516.
[25] V. Augugliaro, T. Caronna, V. Loddo, G. Marcì, G. Palmisano, L. Palmisano, S. Yurdakal, Chemistry: A European Journal. 14 (2008) 4640–4646.
[26] S. Higashimoto, K. Okada, T. Morisugi, M. Azuma, H. Ohue, T.H. Kim, M. Matsuoka, M. Anpo, Topics in Catalysis 53 (2010) 578–583.
[27] C.J. Li, G.R. Xu, B. Zhang, J.R. Gong, Applied Catalysis B: Environmental 115/116 (2012) 201–208.
[28] L. Prieto-Rodriguez, S. Miralles-Cuevas, I. Oller, A. Agüera, G. Li Puma, S. Malato, Journal of Hazardous Materials 211/212 (2012) 131–137.
[29] M. Kositzi, I. Poulios, S. Malato, J. Cáceres, A. Campos, Water Research 38 (2004) 1147–1154.
[30] S. Malato, J. Blanco, C. Richter, M.I. Maldonado, Applied Catalysis B: Environmental 25 (2000) 31–38.
[31] M. Abdullah, G.K.C. Low, R.W. Matthews, Journal of Physical Chemistry 94 (1990) 6820–6825.
[32] J. Colina-Márquez, F. Machuca-Martínez, G. Li Puma, Environmental Science & Technology 44 (2010) 5112–5120.
[33] J.R. Bolton, K.G. Bircher, W. Tumas, C.A. Tolman, Pure and Applied Chemistry 73 (4) (2001) 627–637.
[34] R. Hulstrom, R. Bird, C. Riordan, Solar Cells 15 (1985) 365–391.
[35] R. Marotta, D. Spasiano, I. Di Somma, R. Andreozzi, V. Caprio, Chemical Engineering Journal 209 (2012) 69–78.
[36] C.C. Chusuei, M.A. Brookshier, D.W. Goodman, Langmuir 15 (1999) 2806–2808.
[37] D. Chen, A.K. Ray, Chemical Engineering Science 56 (2001) 1561–1570.